Experimental visualization of inoculation using a charged colloidal model system

Andreas Engelbrecht[1*] and Hans Joachim Schöpe[1*]

[1]Institut für Physik, Johannes Gutenberg-Universität Mainz, Staudingerweg 7, 55128 Mainz, Germany.

*Correspondence to: engelbre@uni-mainz.de and jschoepe@uni-mainz.de

Supporting Information:

Sample preparation

All samples were conditioned in a closed system under inert gas atmosphere. Gas tight tubes connect several devices including a reservoir to add solvent, electrolyte or further particles, an ion exchange column filled with mixed bed ion exchange resin, a conductivity-meter and an optical cell for microscopy (flat rectangular cells of 10x2 mm^2 and 10x1 mm^2 cross section). All optical cell types are made of quartz glass. During preparation the suspension is driven through the circuit by a peristaltic pump. This way the suspension can be kept in a salt free state very efficiently. If the suspension is prepared at particle concentrations higher than the freezing concentration the equilibrium state is crystalline. As colloidal crystals are an extremely soft material the shear induced by pumping melts all crystals and the suspension is transferred into the metastable fluid state. Upon cessation of shear the particles in the metastable fluid readily rearrange forming crystals. The deionization process can be monitored in situ via conductivity measurements. Typical residual ionic impurity concentrations are in the order of the ion product of water. Further details on the preparation have been given elsewhere [1,2].

Crystal growth and determination of metastability

Under fully deionized conditions the equilibrium phase boundary of Pn-BAPS70 suspensions is found at $n_{freezing} \approx n_{melting} = 5.0\mu m^{-3}$. For particle number density exceeding this value the system

crystallizes forming bcc-crystals due to the long ranged nature of the screened Coulomb interaction. The pair interaction energy in monodisperse charged sphere colloidal systems of radius a and effective charge Z^* can be written on the mean field level as: $V(r) = (Z^*e)^2/(4\pi\varepsilon_0\varepsilon_r)\ (exp(\kappa a)/(1+\kappa a))^2\ exp(-\kappa r)/r$ with the screening parameter $\kappa = (e^2/\varepsilon_0\varepsilon_r k_B T\ (n_p Z^* + n_{Salt})\ )^{1/2}$, where $\varepsilon_0\varepsilon_r$ is the dielectric permittivity of the suspension, in this case $\varepsilon_0(0.75\varepsilon_{r,water}+0.25\varepsilon_{r,Glycerol})$. k_BT is the thermal energy at room temperature and $n_{Salt} = 2000N_Ac$ is the number density of monovalent background electrolyte of concentration c with N_A being Avogadro´s number.

The Pn-BAPS70 particles have been used in a number of previous investigations and have been characterized extensively in pure water[3]. Due to deviating physical properties of the water-glycerol mixture the crystallization kinetics is slowed down significantly (decreased NRD, slower growth velocity and higher melting particle number density) in comparison to a purely aqueous suspension.

Crystal growth of crystals heterogeneously nucleated on the container walls were studied by Bragg microscopy using a CCD-camera (piA1900-32gc, Basler, Germany) on a microscope stage (Stemi SV 6, Zeiss, Germany). Here the sample is illuminated with white light under an angle Θ to obtain a Bragg reflection in the direction of the observing microscope objective. The uniformly oriented wall crystals scatter light in direction of the microscope objective if oriented properly to fulfill the appropriate Bragg condition. The resulting color contrast offers the possibility to determine the thickness of the wall crystal as function of time. Further details of this method have been described at length in one of our previous papers[2,3].

The chemical potential difference $\Delta\mu$ between the supersaturated melt and the crystals formed was evaluated from growth measurements of heterogeneously nucleated wall crystals as function

of interaction strength and range. Expressing $\Delta\mu$ in terms of a rescaled energy density $\Delta\mu = B\Pi^*$ with $\Pi^* = (\Pi - \Pi_F)/\Pi_F$ (F denotes freezing)[4] gives the possibility to fit a Wilson-Frenkel law $v = v_\infty(1-exp(-\Delta\mu/k_BT))$ to the measured data with the limiting growth velocity $v_\infty = 7.2 \pm 0.2 \mu ms^{-1}$. The energy density is given as $\Pi = \alpha n V(d_{NN})$, with α being the particle coordination number, $V(d_{NN})$ is the interaction energy at nearest neighbor distance. Using this approach transfers the pair interaction energy $V(r)$ to the chemical potential difference $\Delta\mu$. Further details are given in Ref. 4. This gives us the possibility to connect the particle number density at fully deionized conditions with the chemical potential difference.

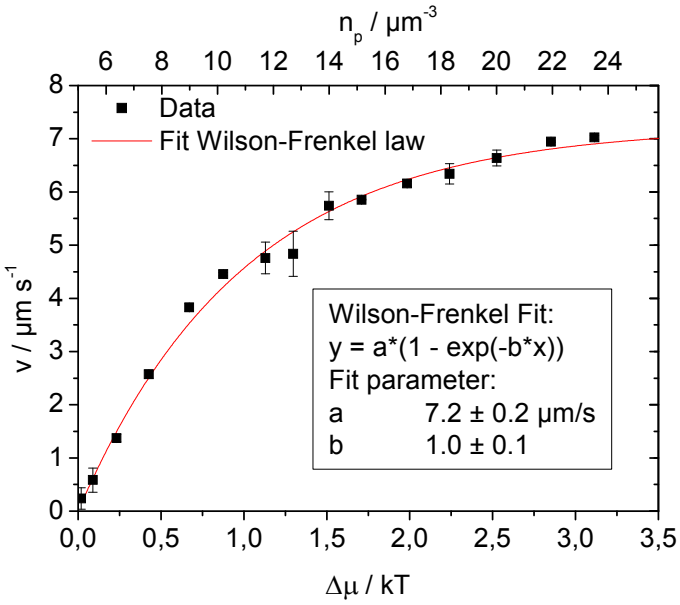

Fig. S1. Crystal growth velocities of oriented crystals of PnBAPS70 particles suspended in 75% water and 25% glycerol as function of particle number density and chemical potential difference. Red curve is a fit to the data according to the Wilson-Frenkel law.

Determination of free remaining volume for nucleation

Figure S2 shows the evolution of the free remaining volume for nucleation, which is necessary for calculation of time resolved nucleation rate densities (Fig. 4, S6). The volume is diminished by nucleation of crystals and their growth afterwards as well as growth of crystals heterogeneously nucleated at the container walls. We calculate the free remaining volume following Wette *et al.*[2]

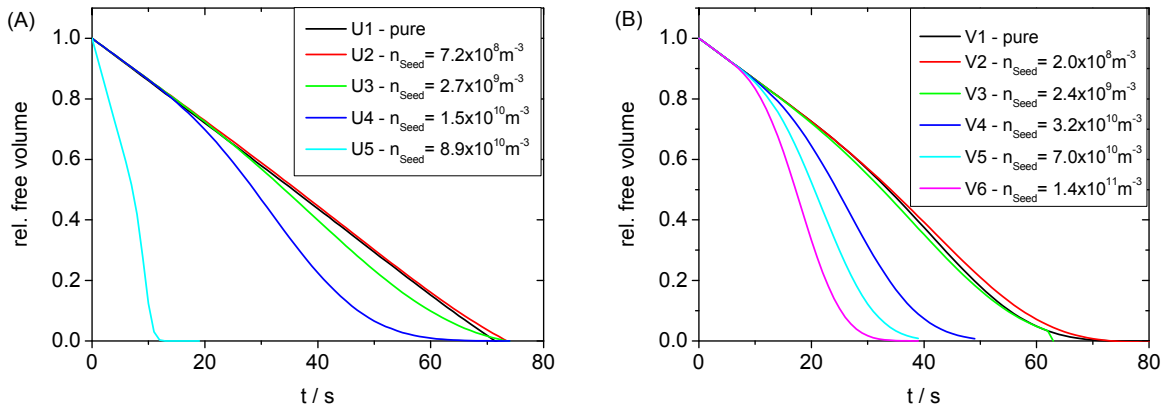

Fig. S2. Time evolution of the relative free volume for (**A**) sample U (n_p=24.7µm^{-3}) and (**B**) sample V (n_p=27.4µm^{-3}) for different amounts of seed addition. Values were calculated by an extension of the KJMA-model[5] by Wette *et al.*[2]

Choice of seed size

Figure S3 illustrates which ratio between seed size and the nearest neighbor distance allows for heterogeneous nucleation and further crystal growth in the investigated suspension of charged spheres.

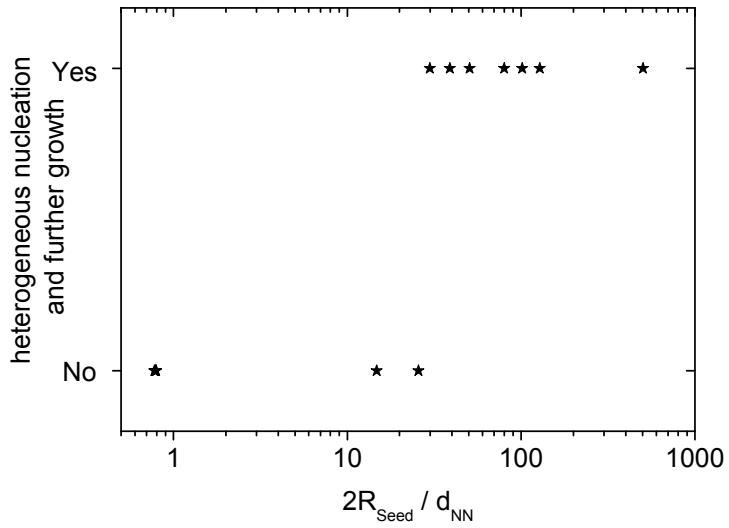

Fig. S3. Heterogeneous nucleation and further undisturbed crystal growth induced by spherical particles as function of seed particle size at a metastability of $\Delta\mu$ = 3.3 k_BT.

Number of individual domains on each seed

As the used seeds are able to nucleate more than just one single crystal on their surface, we counted the number of domains occurring on the seed surface. The results are given in Figure S4: We find a distribution with a maximum around 5 domains per seed. The two dimensional projection of the microscope might lead to a slightly underestimated number of domains per seed.

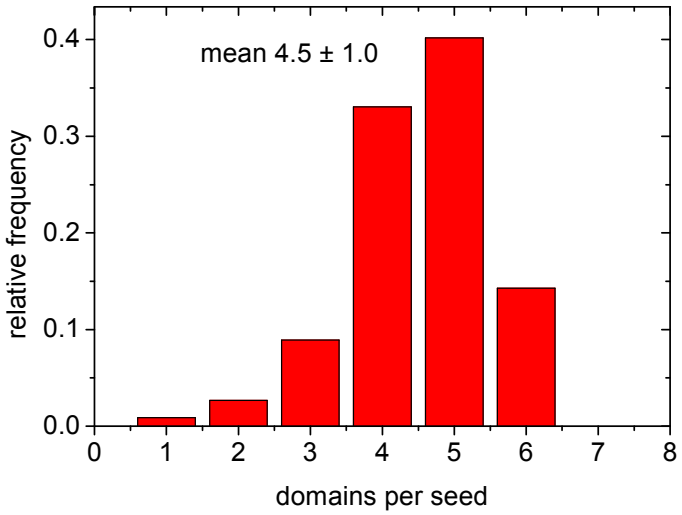

Fig. S4. Distribution of visible crystalline domains nucleated heterogeneously on the surface of the 15.17µm spheres.

Crystal size distribution and time resolved NRD for Sample V

Nucleation kinetics and resulting crystal size distribution of the second investigated sample V (n_p=27.4µm^{-3}) are shown in figure S5 and S6.

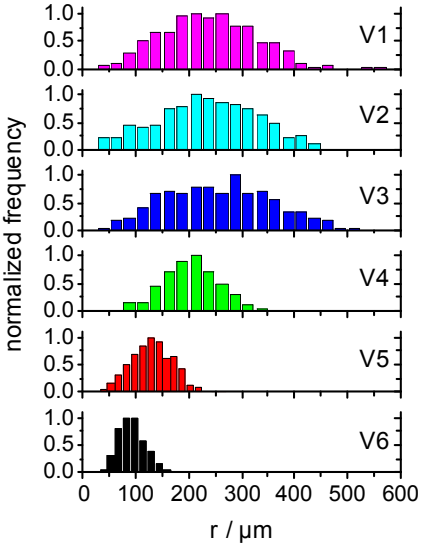

Fig. S5. Distribution of crystal radii for n_p=27.4µm^{-3} after complete solidification obtained from image analysis of polarization micrographs. The seed concentration increases from top to bottom (V1: pure, V2: $n_{Seed} = 2.0x10^8 m^{-3}$, V3: $n_{Seed} = 2.4x10^9$ m^{-3}, V4: $n_{Seed} = 3.2x10^{10}$ m^{-3}, V5: $n_{Seed} = 7.0x10^{10}$ m^{-3}, V6: $n_{Seed} = 1.4x10^{11}$ m^{-3}).

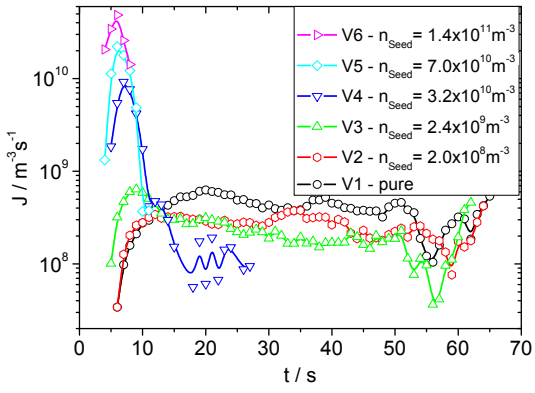

Fig. S6. Nucleation rate densities as function of time n_p=27.4µm^{-3} for different amounts of seed addition.

Analyzing homogeneous and heterogeneous nucleation in the framework of CNT

In classical nucleation theory a spherical growing nucleus must overcome an energy barrier of

$$\Delta G^* = 16\pi\gamma^3 / 3\left(n\Delta\mu\right)^2 = 4\pi\left(3/4\pi\cdot n\right)^{(2/3)}\cdot\gamma\cdot i^{*\frac{2}{3}} + \Delta\mu\cdot i^*$$

in order to keep on growing under energy profit, where n denotes the particle number density of the colloidal suspension, γ the surface tension of the crystal nucleus and $\Delta\mu$ the chemical potential difference between the crystalline and the liquid phase. The number of particles in a critical nucleus i^*, results from the equation $i^* = 4/3\,\pi(r^*)^3\cdot n = 32\pi\gamma^3/3\Delta\mu^3 n^2$. The energy barrier ΔG^* corresponds to the critical radius $r^* = -2\gamma / n\Delta\mu$. Cluster smaller than r^* will decay, while cluster bigger than r^* will grow because the system will decrease its energy. This simple model was first proposed by Vollmer and Weber and was extended by Becker und Döring, Zeldovich as well as Turnbull and Fisher[6,7,8,9]. The growth or shrinkage of the clusters is described by an attachment or separation of single particles. This process can be described using rate equations[Error! Bookmark not defined.,10] and leads to the following result:

$$J = K^+\cdot Z\cdot n_{nucleus}\,.$$

The steady state nucleation rate density is determined by the attachment or condensation rate K^+, describing the attachment of single particles to the crystal nucleus, by Z, the Zeldovich factor which takes the width of nucleation rate barrier into account and by the concentration of critical cluster in the melt $n_{nucleus}$ which is described using a Boltzmann distribution:

$$n_{nucleus} = n_p^{liq}\cdot\exp(-\Delta G^*/k_B T)\,.$$

Here n_p^{liq} is the monomer concentration in the liquid, or the particle number density in the colloidal fluid. The Zeldovich factor is connected with the second derivative of the nucleation barrier and reads like follows:

$$Z = \sqrt{\frac{\left(\partial^2 \Delta G / \partial i^2\right)_{i=i^*}}{2\pi k_B T}} = \sqrt{\frac{\Delta G^*}{3\pi k_B T i^{*2}}} = \frac{1}{8\pi} \frac{n_p^{xtal} \Delta\mu^2}{\gamma^{3/2}} \frac{1}{\sqrt{k_B T}}$$

At the critical size the evaporation rate and the condensation rate are equal and coincide with the maximum of the nucleation barrier height. But a particle attaching to the crystal nucleus has to pass the fluid crystal interface and has to cross an activation energy ΔG_A which is given by the difference in the free enthalpy between the activated cluster $\Delta G(i+1)$ and the unactivated $\Delta G(i)$. The attachment rate for a critical nucleus can therefore described using a Boltzman distribution and follows a form similar to the theory of absolute reaction rates:

$$K^+ = 4i^{*2/3} f_0 \exp(\frac{-\Delta G_A}{k_B T}) = 4 n_p^{xtal\,2/3} \left(\frac{4\pi}{3}\right)^{2/3} \left(\frac{2\gamma}{n_p^{xtal} \Delta\mu}\right)^2 f_0 \exp(\frac{-\Delta G_A}{k_B T})$$

f_0 is the vibration frequency of the particles and n_p^{xtal} is the particle number density of the crystalline nucleus. Assuming that the activation energy can be expressed using the diffusion coefficient D and the interparticle distance in the fluid d_{NN}

$$f_0 \exp(\frac{-\Delta G_A}{k_B T}) = \frac{6D}{d_{NN}^2} \quad f_0 \exp(\frac{-\Delta G_A}{k_B T}) = \frac{6D}{d_{NN}^2} \;,$$

the attachment rate K^+ reads:

$$K^+ = 24 \left(\frac{4\pi}{3}\right)^{2/3} \left(\frac{2\gamma}{n_p^{xtal} \Delta\mu}\right)^2 \frac{D}{d_{NN}{}^2} n_p^{xtal\,2/3} = 24 \left(\frac{4\pi}{3}\right)^{2/3} \left(\frac{2\gamma}{\Delta\mu}\right)^2 D\, n_p^{xtal\,-4/3} n_p^{liq\,2/3}$$

By connecting all the different equations one arrives at the final result for the nucleation rate density:

$$J = 12 \left(\frac{4}{3}\right)^{2/3} \pi^{-1/3} \sqrt{\frac{\gamma}{k_B T}} \cdot D \cdot n_p^{xtal\,-1/3} \cdot n_p^{liq\,5/3} \cdot \exp(-\Delta G^* / k_B T)$$

In monodisperse charged colloidal systems under fully deionized conditions, the particle number density of the crystal and the fluid are equal and so one end up with the following expression:

$$J = 1.55 \cdot 10^{11} \cdot n^{4/3} \sqrt{\gamma} \cdot D_S^L(n) \cdot \exp\left(\frac{-16\pi\gamma^3}{3k_B T (n\Delta\mu)^2} \right)$$

The long time self diffusion coefficient close to phase boundary does not vary with n [11] and is given by $D_S^L = 0.1 D_S^S$,where $0.1 D_S^S$ is the short time self diffusion coefficient determined by dynamic light scattering. As n, $\Delta\mu$ and D_S^L are known the numerical expression provided by CNT can be used to calculate the surface tension γ and thus the nucleation barrier height ΔG^*.

In the case of heterogeneous nucleation theory the nucleation barrier height is reduced by the catalytic factor f: $\Delta G^*_{het} = f \Delta G^*_{hom}$. If heterogeneous nucleation occurs an planar wall classical theories[10] predict a spherical crystalline cap on the substrate and the catalytic factor only depends on the contact angle Θ between the substrate and the nucleus: $f(\Theta) = \frac{1}{4}(2-3\cos\Theta+\cos^3\Theta) \leq 1$. In the case of heterogeneous nucleation on spherical substrates $f = f(\Theta, R_{seed}/r^*)$ becomes a complex function of the contact angle and the ratio of seed size to critical nucleus size[Error! Bookmark not defined.]. Further details are given elsewhere[12,13].

The kinetic prefactor is given by the attachment rate and by the Zeldovich factor. Assuming that the long time self diffusion coefficient responsible for the single particle attachment in the homogeneous and heterogeneous nucleation process are equal the kinetic prefactor for homogeneous and heterogeneous nucleation can be presumed to be identical. This gives the possibility to calculate the difference between the homogeneous and the heterogeneous nucleation barrier height: $\Delta G^*_{hom} - \Delta G^*_{het} = \ln[(J_{het}/n_{Seed})/(J_{hom}/n_p)]$ an thus the catalytic factor as the absolute value of ΔG^*_{hom} is known. The following table gives an overview of the obtained results:

sample	$n_p/\mu m^{-3}$	$J_{hom}/m^{-3}s^{-1}$	$\Delta G^*_{hom}/k_BT$	R_{seed}/r^*	$\langle J_{het}/n_{Seed}\rangle$	$\Delta G^*_{hom} - \Delta G^*_{het}$	f
U	24.7	$2.2x10^7$	31.63	13.18	0.3	26.64	0.16
V	27.4	$4.6x10^8$	28.77	14.63		23.75	0.17

Movie 1. Crystallization of the pure suspension at $n_p=27.4\mu m^{-3}$

Movie 2. Crystallization of the suspension at $n_p=24.7\mu m^{-3}$ and a seed concentration of $1.5x10^{10}m^{-3}$.

1 A. Engelbrecht, H. J. Schöpe, Crystal Growth & Design, 2010, 10, 2258

2 P. Wette, H. J. Schöpe, T. Palberg, J. Chem. Phys., 2005, 123, 174902

3 A. Engelbrecht, R. Meneses, H. J. Schöpe, Soft Matter, 2011, 7, 5685

4 M. Würth, F. Culis, J. Schwarz, P. König, T. Palberg and P. Leiderer, Phys. Rev. E, 1995, 52, 6415

5 M. Avrami, J. Chem. Phys., 1939, 7, 1003; 1940, 8, 212; 1941, 9, 177

6 M. Volmer, A. Weber, Z. Phys. Chem., 1926, 119, 227

7 R. Becker, W. Döring, Ann. Phys., 1935, 24, 719

8 D. Turnbull, J. C. Fisher, J. Chem. Phys., 1949, 17, 71

9 J. Zeldovich, J. Exp. Theor. Phys., 1942, 12, 525

10 *Handbook of Crystal Growth,* ed. D. T. J. Hurle, Elsevier, Amsterdam, 1993

11 F. Bitzer et al., Phys. Rev. E, 1994, 50, 2821

12 N. H. Fletcher, J. Chem. Phys., 1958, 29, 572

13 M. Qian and J. Ma, J. Chem. Phys., 2009, 130, 214709